— 2018 NASA BIG Idea Challenge —

Utilization of Solar Cell Umbrellas to Provide Long-Term Photovoltaic Power on Mars

Texas A&M University

Team Members:
Gabrielle Adams, Joshua Banks, Cole Frazier, Uday Toodi

Faculty Advisor:
Ms. Magda Lagoudas

20 February 2018

Summary: In order to make a manned mission to Mars possible, a consistent power source must be developed for deployment on the Martian surface. This report will explore utilization of an Applied Photovoltaic (PV) Power Array (APPA) for power generation on Mars. APPA involves the deployment of four umbrella-like structures covered in flexible, thin film solar cells. These umbrellas will be installed on a rectangular lander with electromagnetically actuated booms that deploy the system autonomously. Tethers connected to vertical pillars on the lander will provide additional support for the boom structure. Carbon fiber reinforced materials and Polyether Ether Ketone (PEEK) are recommended for use for the majority of the structural components, including the umbrella supports, for their lightweight yet high strength properties. To minimize solar cell weight, triple junction $GaInP_2$/GaAs/Ge solar cells adhered to interwoven Kevlar/carbon fiber fabric act as the PV power producing element of the array. This highly-flexible design fulfills the packing needs of the umbrella. An omnidirectional anti-reflective coating increases the light capturing abilities of the solar cells, increasing its efficiency. As a means of active dust abatement, an electrodynamic system is implemented to electrically pulse accumulated dust off the array in conjunction with the passive dust abatement afforded by the curvature of the umbrella. APPA's structural stability is validated through FEA conducted on the boom and the umbrella. The power produced by the array is assessed in VR models accounting for dust accumulation, incidence angle calculation throughout the day, and power generation for the triple junction cells.

1. Introduction

As interest in Mars pushes humanity closer towards sending a fully manned mission to the surface of the planet, numerous challenges must be addressed; power generation is of particular importance. As solar energy is a relatively abundant source of energy, utilization of solar arrays is perhaps the most feasible renewable method of solving this issue. Even so, numerous challenges stand in the way of solar power generation on Mars.

In this report, a novel concept to employ a solar array on the surface of Mars in support of a manned mission will be detailed. This work has been inspired by NASA's Breakthrough, Innovative, and Game-Changing (BIG) Idea Challenge, a competition designed to allow student-led University teams to pursue creative avenues of design to solve some of the biggest engineering challenges posed by space exploration and settlement. For this report, the proposed design has been created by a team at Texas A&M University in College Station, Texas, with aid from faculty sponsor Dr. Lagoudas along with other notable faculty support.

First, the report will present our proposed solar array design, the Applied Photovoltaic Power Array (APPA). The main structure and its deployment will be detailed, followed by the solar cell design and specific mechanisms and components. Dust abatement methods will also be presented. Next, the report will examine validation performed to prove the feasibility of APPA, including FEA and models created to analyze power production capabilities. APPA represents a novel solar array design that meets many critical design requirements which makes it a viable design solution for NASA.

2. Design Concept

In this section, the design of APPA is detailed. First, the overall structure and its components - along with the autonomous deployment methods - are examined. Next, the solar cell design, including substrate selection, cell type, and protective coatings follow main structure design. Finally, details of mechanisms and components which support the overall proposed design are presented.

2.1. Main Structure and Deployment

The overall concept of the solar array is to deploy large solar cell umbrellas above the Martian surface. Renditions of the packed, intermediate deployment, and fully deployed arrays are shown in Figures 1 and 2, respectively. In our design, four umbrellas of 18 m diameter are used to fulfill the 1000 m^2 surface area requirement. To allow full extension of an umbrella without interfering with any other structures, the umbrellas will be deployed nearly 12 m from the lander using booms actuated by electromagnetic forces and supported by tethers. Each umbrella array is connected to a lander-centric pulley system which would provide the means to deploy each umbrella's solar cells. When deployed, the entire assembly is symmetrical with a low center of gravity, thereby providing stability throughout deployment.

Figure 1: *Packed lander assembly with base dimensions of 1.5m by 1.5m and height of 4.4m.*

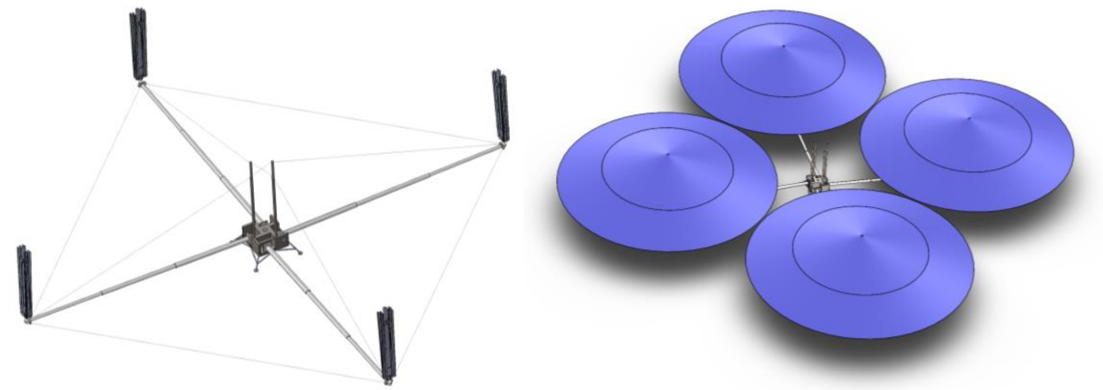

Figure 2: *Extended booms with stowed solar arrays (left) and with deployed solar arrays (right).*

2.1.1. Solar Cell Umbrella Design

The heart of the design revolves around the utilization of solar cell umbrellas as the primary infrastructure for photovoltaic power generation. Each umbrella employs a central shaft and six extending arms created by a series of interlocking links - similar to the design of a collapsible umbrella - as the means to deploy a fabric material with embedded solar cells. The top cuff would deploy downward, with help from gravity as well as a pulley system and would lock in place once it reached the fully deployed position. At that time, a tether attached to the end of the arm and top of the central shaft would be fully in tension and would support the fabric of the solar cells. Figures 3 and 4 below showcase the stages of the umbrella unfolding mechanism along with indications of the subcomponents.

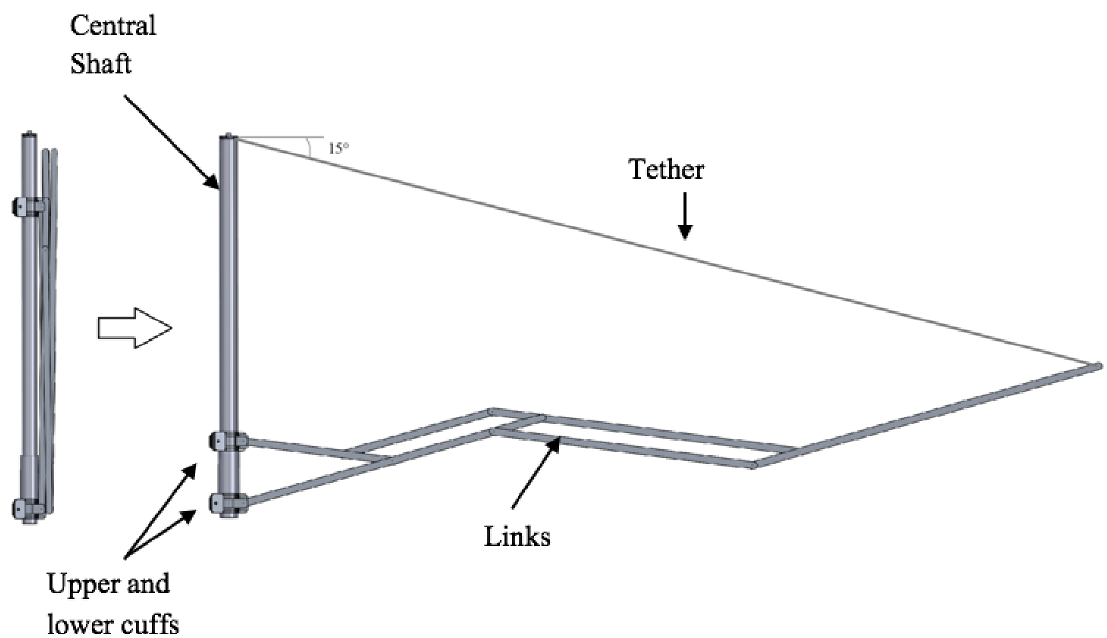

Figure 3: *Unfolding mechanism of one umbrella arm*

Figure 4: *Umbrella design in the open position with tethers to support solar cells.*

Each set of arms is connected to the shaft by a rotating cuff, which allows compact storage of the umbrella as the arms can collapse upon one another during space transportation. In total, the diameter of the roughly conical solar panel surface is 18 m, while the shaft itself stands at 4 m tall. The links making up the structure are of various lengths, ranging from 1.625 m to 3.75 m. Each umbrella would contain a solar panel surface area of about 255 m^2 which yields a combined 1020 m^2 surface. Figure 5 demonstrates the functionality of the rotating cuffs from open to close.

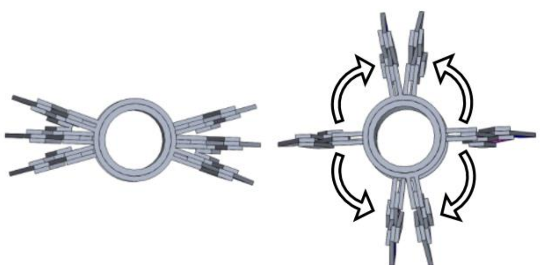

Figure 5: *Top view of upper and lower cuffs when stored (left) and when in deployment position (right)*

On the left image of Figure 5, it is seen that the stowed configuration takes up less space in the vertical position. This is done by having the cuffs rotate independently about the central shaft. Motion is induced using torsional springs and pin-hole locking mechanisms secure the cuffs once the position reaches the fully deployed state. This is done before the links are expanded outward to help with the fluidity of the fabric unfolding and reduce inertia of the arm assembly rotation.

A deployed slope on the solar panel surface of 15° from horizontal provides at least a small advantage for passive dust abatement when compared to a flat panel such as the ones found on the Phoenix lander [1]. The flexibility of the solar cells allows them to be stored between the arms when closed. This design will require compact packing of the solar cell material. An exact folding design and deployment scenario was not determined, however a simple geometry and panel volume evaluation confirms there is sufficient space for storage. A subscale prototype will be generated in a later phase of this project to further define the solar cell fold, store and deploy designs.

2.2. Boom Design

In this section, the design of the booms which support the solar umbrellas is discussed. First, an overview of the boom will be provided. Next a discussion of the material selection for the boom will provide a basis for the manufacturing processes proposed. This is followed by a discussion of the deployment of the booms to positions that allow the solar cell umbrellas to open.

2.2.1. Boom Overview

To facilitate the spacing of the solar umbrellas, four telescoping booms will be used to position each umbrella approximately 12 m away from the lander base. In the stored configuration, the booms align vertically on the lander (Figure 1) and rotate 90° to a horizontal configuration. Each stage of the boom has an elliptical cross section. This geometry would mitigate rotation due to torsional loads as compared to a circular cross section. It also reduces stress concentrations around the perimeter of the boom due to the absence of sharp geometry (e.g. corners).

Each telescoping boom is comprised of three stages, where each stage is 3.75 meters in length. The first stage is closest to the lander, the second is the middle section of the boom, and the third would be the farthest away, directly supporting the umbrella load. These booms will be supported by a series of tethers, discussed below and seen visually in Figure 2.

2.2.2. Material Selection

To minimize mass without compromising strength and durability, high performance materials such as Polyether Ether Ketone (PEEK) and carbon fiber reinforced polymers can be used for both the boom and the umbrella infrastructure. These materials also provide flexibility in the choice of manufacturing. Materials like PEEK provide excellent properties such as high strength and hardness, flexural strength, and fatigue resistance. Carbon fiber reinforced polymers also exhibit similar, but not as robust, properties as PEEK with a lower mass. The simulations run for the analysis of the boom utilized the properties of carbon fiber reinforced polymers.

A potential manufacturing process that can be used is Essentium Materials' FlashFuse™ technology [2]. FlashFuse brings in-situ electrical welding processes to 3D printing. FlashFuse uses filament coated with conductive carbon nanotubes to weld each printed cross section to the previously printed layers. By addressing the bonding of the polymer chains at the nanoscale level, larger heat affected zones are created, thereby improving the strength of the cross sectional welds and the resulting strength of the parts. FlashFuse improves the isotropic mechanical properties of the part when compared to traditional 3D printing methods. Using FlashFuse increases the amount of time the polymer chains have to migrate and entangle. This reduces internal stresses that are in the end product and resolves interlayer delamination issues, allowing for lightweight, yet strong, materials to be used in the boom. Additionally, should the boom stages be constructed in stages, this would allow for parts to be 3D printed by astronauts on Mars. This kind of modularity allows for flexibility in design, long term use, and maintenance.

2.2.3. Deployment/Actuation

To deploy the stages of the boom, electromagnetic force, akin to a coilgun, will be used. Lorentz forces will be generated when a current is sent through a coil of wire embedded in the first and second stages of the boom structure. With the implementation of space-grade bearings similar to ball-transfer-units, the acceleration required to successfully extend the boom is achieved.

The load that is transferred by the actuation to the second and third stage would provide an acceleration of 0.2 m/s^2. Using the coefficient of friction in the bearings [3], the frictional force that must be overcome to initiate movement would be approximately 615 N (with respect to Earth's gravity), considering that the mass of the total moving load is approximately 627 kg. Therefore, the total force required for actuation would be approximately 630 N, with respect to Earth's gravity.

Figure 7: *Boom assembly mid-deployment*

Figure 7 illustrates the boom deployment. Lorentz forces are generated when a current moves through a conductive wire, generating a change in the electromagnetic field. The Lorentz force is calculated using Equation 1. To generate this force, a coil of 269 turns is proposed to be used on both the first and second stages of the boom. This would allow for stages two and three to deploy in tandem, then stage three moves to the final position. For this estimation, 300 kcmil copper wire was used in the calculation for the current required. From the resulting calculations, the current required for the actuation is approximately 83 A. To provide this current, a bank of ultracapacitors will be used to discharge the required energy. Equations 4 and 5 relate the work required for the boom deployment to determine the capacitance required (1948 F). In these equations, C is the capacitance (Farads), V is the voltage (Volts), R is the resistance (0.3146 ohms) based on the above wire specifications, and I is the current required as specified by Equation 3. The ultracapacitors used can either be pre-charged, or a battery bank can be used in tandem to allow for reliable charging and discharging.

$F = I(L \times B)$ (Equation 1)

$B = \frac{\mu_0 N I}{2r}$ (Equation 2)

$I = [\frac{2Fr}{\mu_0 N}]^{1/2}$ (Equation 3)

$Fd = 0.5CV^2$ (Equation 4)

Where:
$V = IR$
d = 3 meters

2.3. Arrangement & Packing

Based on the 1000 m^2 surface area requirement of the umbrella along with the 10 m^3 volumetric limitations of the stowed array, four solar cell umbrellas will be stored inside of one lander. As shown in Figure 8, each telescopic boom will be oriented 90° relative to one another in a cross like pattern when deployed. These booms will be folded upwards when in the stored position, then rotate 90° downwards to create this cross shaped deployment pattern. Thus, the overall shape of the stowed array is a square prism with side lengths of 1.5 m and a height of 4.4 m. The boom-umbrella assemblies will be tethered to large pillars next to the assemblies, keeping them secure throughout flight and storage. Once the lander has safely landed on Mars, these tethers will slowly lower the boom down until it is parallel to the planet surface. Cut-outs of the lander base will act as a seat for the boom. A shaft is run through circular connections attached to the back plate of the boom, acting as a rotation point during the lowering process. Once deployed, the tethers will lock into place and act as vertical supports for the boom assembly.

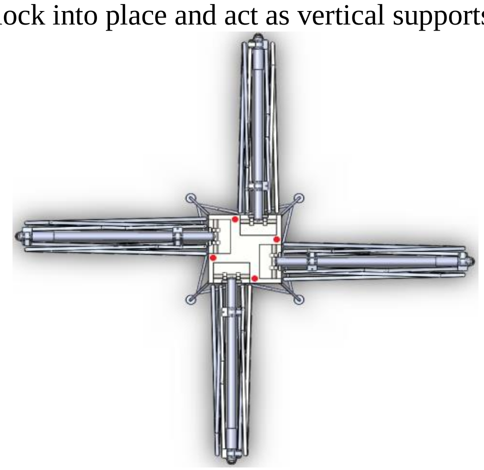

Figure 8: *Top-down view of post-deployment orientation relative to the lander. Each red circle represents a structural pillar for tethering to its corresponding boom.*

During storage, each boom-umbrella pairing takes up a maximum of 2 m^3, occupying a total volume of 8 m^3 for all the boom-umbrella assemblies. Similarly, the pillars inside the lander take up another 0.108 m^3, leaving 1.092 m^3 of volume unused by the primary array components inside the lander. This space will be used to house the auxiliary components necessary to make the array function including batteries, cables, or other electronics. The design of these specific components are out of the scope of this project, but their consideration in terms of lander space potential is necessary and present inside of our design.

2.4. *Tethers and Pulley System*

To provide structural support, a system of tethers will be utilized. The tethers, made of 12-strand single-braid Kevlar rope will be secured at the end of the booms to the central pillars of the lander. The choice of Kevlar cables allows for significant strength with low mass. Kevlar rope retains strength even at low temperatures. By using an epoxy resin coating, the rope can be protected from UV rays posed by the Martian environment. As the angle of the tether to the central pillar is quite acute, it is necessary that a hole be manufactured into the umbrella fabric to provide the crucial support the tether offers. The largest diameter of such a hole would be 0.0254 m, which results in a removed area of 5.07×10^{-4} m^2. Such a small area, especially when placed outside of a solar cell grouping, would not likely result in serious stress concentrations or losses in power generation.

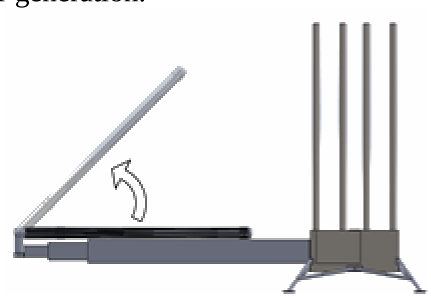

Figure 9: *Umbrella assembly packaged on top of the boom*

To deploy the umbrella structure from the boom, an integrated pulley system will be used to pull the top of the umbrella from the stored position to an upright, deployed position. This can be facilitated with a motor integrated at the base of the umbrella. The motion would be similar to that of a kneecap, allowing for a 90° sweep of the umbrella structure as shown in Figure 9.

2.5. Solar Cell Design

In this section, the overall PV power production design is outlined in two sections First, the selected solar cell type is described. Next, the infrastructure behind its deployment and the coating designed to maximize power production are outlined. Later in the report, the power production capabilities of APPA are outlined along with the underlying methodologies behind the calculations.

2.5.1. Overall Design

When considering what solar cell type to choose, numerous factors were taken into account. The challenge requirements presented significant obstacles to any cell type, most notably the long service life and weight demands. While power production requirements were not expressly given, a solar cell with superior efficiency is obviously favorable. Similarly, a flexible cell capable of conforming to a unique panel shape driven by the umbrella design also presented a requirement unique to this design. With all of these competing requirements in mind, an inverted metamorphic multijunction (IMM) cell was selected.

IMM cells utilize germanium (Ge) as the base material paired with three independent p-n junctions, each of unique materials. The major advantage of these variable junctions is the flexibility it provides in terms of light absorption capabilities, as each junction is made of different materials optimized for a particular portion of the wavelength spectrum. As a larger range of the light spectrum is more significantly utilized, the inherent efficiency of the cell improves, surpassing all other current cells [4-5]. Along with a high degree of design flexibility, the cells are thin with a thickness typically below 250 µm. With a reduced thickness also comes lightweight properties, operating at a mass around 75 mg/cm^2, considerably lower than silicon based cells. The operating lifetime of currently manufactured IMM modules can reach 25 years, avoiding the degradation properties that plague organically-based solar cells [6]. For all of these reasons, triple-junction IMM solar cells were selected as the power production source for APPA.

A product produced by Spectrolabs currently used in space application was selected as the cell of choice. The three junctions are $GaInP_2$/GaAs/Ge. Cell weight is 50 mg/cm^2 and cell thickness is 80 µm. Each cell is oriented in a rectangular configuration, taking up an area of 27 cm^2. Efficiency for the cell under standard conditions is 30.7%. Information regarding open circuit voltage, short circuit current, and maximum power points are also provided at standard conditions for Earth [7]. To help orient this information to Martian conditions, adjustments to cell properties under varying temperature is another given parameter in the data sheet, which will be discussed in the performance based section of the paper.

2.5.2. Infrastructure and Coating

A highly flexible, lightweight, and robust solar cell infrastructure must exist to fulfill the needs of the umbrella during storage and deployment. Solar cells rooted in a fabric-like design provide both the flexibility and lightweight properties necessary for space application. Although the technology is not mature, many researchers have produced viable prototypes. For example, testing of solar cell fabric resistance to cyclic bending has produced promising results, as little change to cell efficiency occurred over 100 bending cycles [8].

There are three methods to produce solar cell fabrics. One approach involves pre-produced solar cells adhered to a fabric surface under a number of different techniques. The second is a solar cell printed onto the fabric itself, making it a part of the overall structure of the solar cell. The third solution involves solar cell threads woven into a fabric, making the textile the cell itself [9]. Although solar cell threads sound promising, research shows that in practice the weaving process damages the cells, limiting its potential output before power collection even occurs [10]. Similarly, direct printing of a solar cell onto the fabric must be completed in a low temperature manufacturing process, limiting its potential to organically based cells. Thus, adherence of the cell to the fabric itself is currently the only viable option, either through a lamination or welding technique [11].

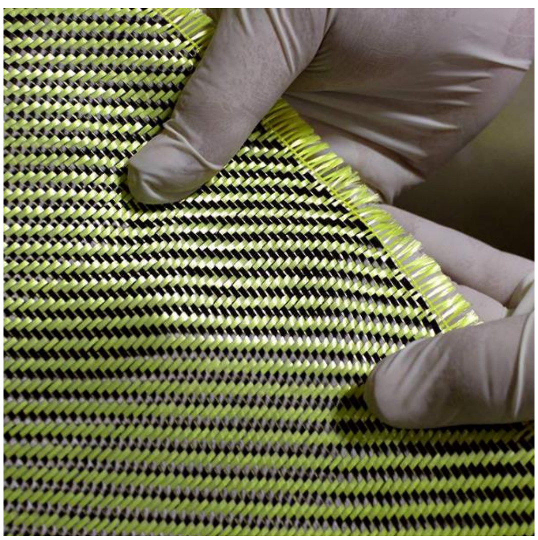

Figure 11: *Fabric chosen as the substrate for the solar cells, illustrating the combined Kevlar/Carbon fiber threads [10].*

In order to withstand the high temperature manufacturing process of adhering the cell to the fabric, a material that is capable of withstanding a hot environment must be selected. A high degree of mechanical strength is also required to withstand the long mission duration and stress of added solar cell weight. To meet these demands, a combined Kevlar and carbon fiber fabric was selected as the material of choice for their ability to provide structural integrity under the high temperature lamentation process along with representing the highest strength fabrics on the market. Produced by Fibre Glast, the fabric weighs 180 g/m^2 at a thickness of 280 um [12]. The fabric is also woven in a twill pattern, which provides a smoother surface and high inherent mechanical properties than plain weave. In the twill weave, Kevlar is oriented in one direction while carbon fiber is oriented in the other, perpendicular to the Kevlar weave. Figure 11 illustrates the fabrics design.

To provide a conductive surface for power flow, reduce porosity of the fabric, and increase strength, a layer of titanium will be applied on top of the fabric [10, 13]. The layer of titanium will be 1 µm in thickness, adding 4.5 g/m^2 of weight to the fabric. Layered onto the titanium layer, the solar cells will be adhered to this corresponding substrate. As an addition to the triple junction solar cell, a 4-layer anti-reflective coating (ARC) is implemented to reduce losses from light reflection and scatter. This coating is comprised of 4 independent layers of SiO_2 and TiO_2 deposited under unique sputtering techniques and deposition angles, specifically designed for improving triple junction cell performance. The 4-layer ARC has a total weight of 1.5 g/m^2. Under laboratory conditions, the ARC saw an average improvement in light transmittance of 35% over a cell with no coatings, with exponentially improving gains as incidence angle increases [14]. These results point to the omnidirectional properties of the ARC, especially beneficial in a Martian application due to the high degree of light scatter from suspended dust particles in the atmosphere. Figure 12 displays similar results with open circuit voltage and short circuit current.

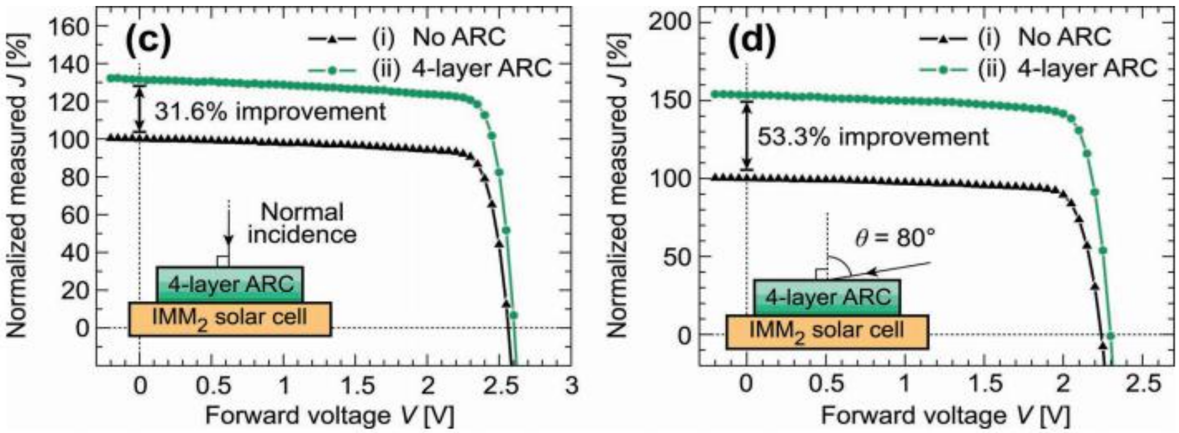

Figure 12: *Open circuit voltage and short circuit current improvements with application of a 4-layer ARC versus a cell without any coating [12].*

To finalize the solar cell fabric, an epoxy resin with low refractive index properties acts as the lamination material, adhering the entire structure together. This epoxy layer provides mechanical improvements and physical protection of the ARC layer and solar cell itself from the Martian elements. Similarly, the epoxy protects the underlying Kevlar fabric from any potential UV light exposure, the dangers of which were described previously in the tether section. A thickness of 76.2 µm on each side of the fabric is used, as this both provides protection from the elements yet still flexible enough to be bent [15]. In total, the solar cell fabric, including cell, fabric, titanium, and ARC has a weight of 866 g/m^2.

2.6. Dust Abatement

The Martian environment provides additional challenges of dust abatement on the system design. The Martian surface is covered with a fine sand that is subject to electrostatic charging. This causes the particles to stick on surfaces similarly to how polyethylene food wrap works. In order to combat this challenge, past solar equipment like the Martian Exploration Rovers relied on cleaning events, during which wind would blow off dust and restore solar power generation [1]. The curvature of APPA's solar umbrellas would create favorable angles of incidence for these passive cleaning events, resting at 15 degrees below the horizontal. However, this method alone would not be appropriate for supporting a future manned mission as solar power is imperative to human survival. In order to supplement this passive dust abatement, a transparent electrodynamic system (EDS) is proposed as an active approach.

EDS provides active dust abatement by using electrostatic forces to remove the charged particles from the array surface. This system uses phased voltages and electricity to create an electrostatic wave that repels the dust particles. This can be created by printing conductive materials within a transparent layer that receives meticulously choreographed pulses of energy. This transparent layer would then be added like a film on the surface of the solar panels. Preliminary results suggest that this system can remove 90% of deposited dust [16]. This concept has been suggested for regions on Earth, like the Middle East, where arid and sandy environments cause similar problems for solar power generation on Mars. While testing has only been completed on Earth environments, the technology shows great potential for the Martian application. It is lightweight and requires a relatively small amount of power.

The plot shown in Figure 13 is for a test panel of 59 cm^2. It is clear that the efficiency begins to plateau between 3 or 4 mW. In order to optimize the tradeoff between power requirements and panel efficiency gained, a power of about 4 mW would be proposed for this specific panel. This same article also suggest that a 1 m^2 panel would require 5 W, not including the no load power condition for the power supply. For larger panel sizes, there is more dust to remove and the dust has to travel farther to be properly displaced. It is also important to understand that there are various other factors that are involved in determining the power requirements for the EDS.

This includes whether the system is operated continuously or intermittently and the excitation frequency, both of which should be optimized for the given panel arrangement. Making an assumption that this would scale linearly, the power needed to operate one umbrella's EDS would be 1.3 kW. While this is not entirely accurate, this gives enough validation to show that the EDS would only use a very small fraction of the overall power generation. The dust model generated and detailed in the performance section of this report can be used in the future to better define the parameters chosen for the EDS.

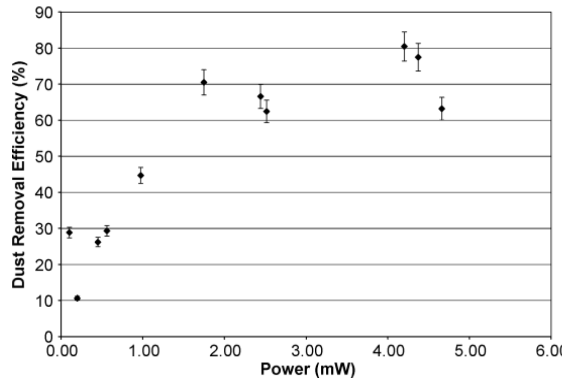

Figure 13: *Efficiency of a continuously run EDS on a 59 cm^2 test panel at various overall power consumptions [16].*

3. <u>Validation</u>

In order to have a successfully deployable solar array, the array must be able to withstand the impact forces of landing as well as the transient forces associated with the deployment process. It is important to show that the structure is adequately supported during every stage throughout deployment. Additionally, the structure must be able to survive under varying static loads for the product lifetime of 10 years. For these stress analyses, the Solidworks Simulation FEA program is used to solve the more complex geometries and load patterns. Properties of carbon fiber reinforced materials were used for these simulations. Additionally, it is important to show that all aspects of the design withstand the thermal cycling present day to day on Mars. These validations are done in the following sections.

3.1. FEA Analysis

In order to show structural integrity during the deployment process, the boom assembly is analyzed. In this analysis (Figure 14), the weight of Earth's gravity acts at the center of gravity, the loads of the umbrella infrastructure (225 kg), the solar cells (150 kg) and the solar cell fabric (216.5 kg) act downward on the end of the boom while a tethering force acts upward and towards the lander at an 18.54° angle.

As is evident with the FEA, the largest stress occurs in the third stage. Stresses of approximately 6 MPa are significant, but do not exceed the flexural strength of the carbon fiber reinforced material (Flexural strength of 165 MPa). This shows that the segment of the boom should be redesigned to provide optimum support. Additionally, material properties for finalized materials should be used in future analysis.

Furthermore, carbon-nanotube composites of PEEK and other high-performance materials that can be used with technologies like FlashFuse have yet to be investigated for material properties. It is expected that by 2030, such research and development will be completed and implemented for manufacturing use, allowing for more detailed analyses to be conducted.

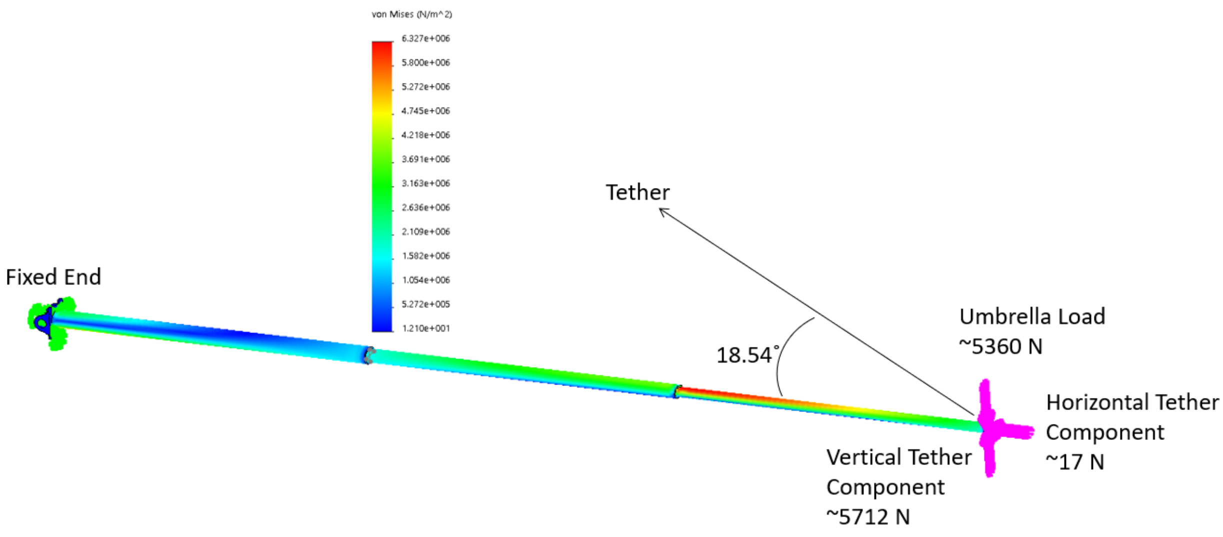

Figure 14: *Results of fully deployed boom FEA.*

Additionally, the links in the umbrella array must be strong enough to support the fabric, their own weight, and any wind loading; they must also be lightweight and compact. In this sense, the FEA was used not only to validate the structural integrity of the umbrella design, but also to optimize the mass and size properties. Material was able to be removed when the stress was less critical, improving the mass to strength efficiency of our design, but further optimization to reduce weight could be performed.

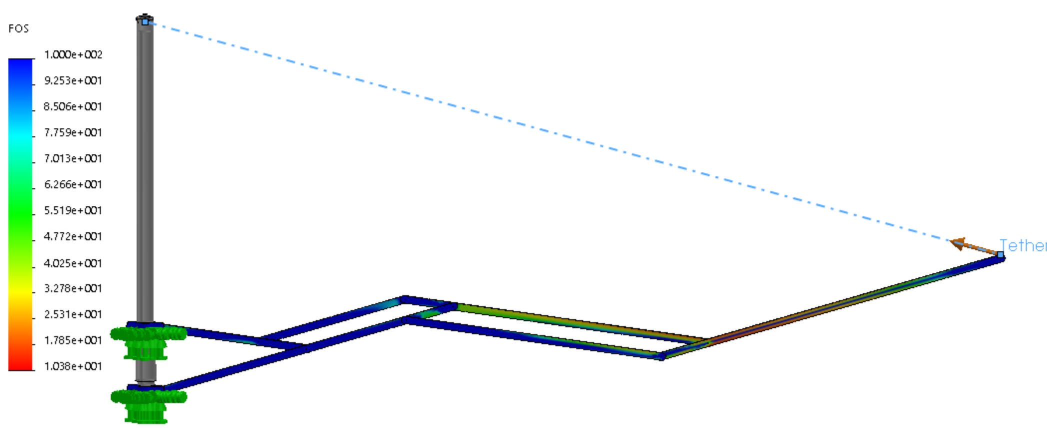

Figure 15: *Fully deployed umbrella arm static FEA.*

As seen in Figure 15, the final design iteration of the umbrella link arm assembly has a factor of safety of 10. This was assessed by assuming that each of the 6 umbrella arms supported ⅙ of the fabric weight, about 280 N, and the distribution of this weight correlated with the cell area. The weight of the links, approximately 320 N in total, was also taken into account again using Earth gravity as a worst case scenario for deployment. The tether was represented by a point load whose force was determined by simplified statics calculations. This same analysis was done halfway through deployment and at the end of deployment right before the tether gained tension. In practice, as the deflections increase during deployment, the tether will gain some tension via the pulley system before the final stage providing some support throughout. Overall, this validation shows that the structure will support the necessary loading during all stages and with minimal deflection.

3.2. Thermal Analysis

Due to the large amount of thermal cycling that occurs on Mars, another important design consideration in the validation process is the solar array's ability to withstand thermal fatigue. During the design embodiment process, special care was taken to choose structural materials that performed well at low temperatures and had low thermal expansion coefficients. As previously discussed, some high-performance materials such as PEEK and carbon fiber reinforced materials have exceptional thermal and mechanical properties, reducing the effects of thermal cycling.

An additional consideration that should be factored is the ductile-to-brittle transition temperature (DBTT) for the material. With temperatures as low as -100 ˚C, the DBTT will likely be passed and the material will behave in a brittle manner. To avoid catastrophic failure that is associated with brittle materials, resistive heaters can be embedded and used throughout the boom to maintain a viable operating temperature. During deployment, this DBTT will likely not be passed thereby not requiring such heating during deployment.

Additionally, the solar panels themselves are required to maintain good performance during thermal cycling. In order to assess the thermal stresses induced within the panel, the strain due to varying thermal expansion coefficients between the fabric and the cell could be addressed. For the purpose of this evaluation, it is assumed that the solar panels are assembled in an environment of 100 °C. This estimate was made based on the manufacturing process and allows for negligible residual stresses at 100 °C. Stress in induced whenever the temperature deviates from this datum, which will occur during the prescribed cycling conditions (-100 to 25 °C). However, the thermal expansion coefficients for these materials were all very small so the resulting strain, and thus stress, would be minimal.

4. <u>Performance</u>

4.1. Spacecraft Sunlight Model

Since the current SpaceCRAFT VR environment takes place in a fixed-planar coordinate system, making the planetary environment orbit around the sun was infeasible. Instead, the sun was rotated about the surface, creating a path across the sky that simulated the different seasons of Mars. The sun rotation model, showcased in Figure 16, took into account the latitudes, year length, distance from the sun, and tilt angle of the planet. The distance from the sun to Mars was important in this model as it would affect the incidence angles on the solar panels and thus the simulated efficiency of our array. Additionally, the daily and yearly Martian solar surface fluxes were used in within this model to help analyze theoretical solar array performance in a precise manner [17].

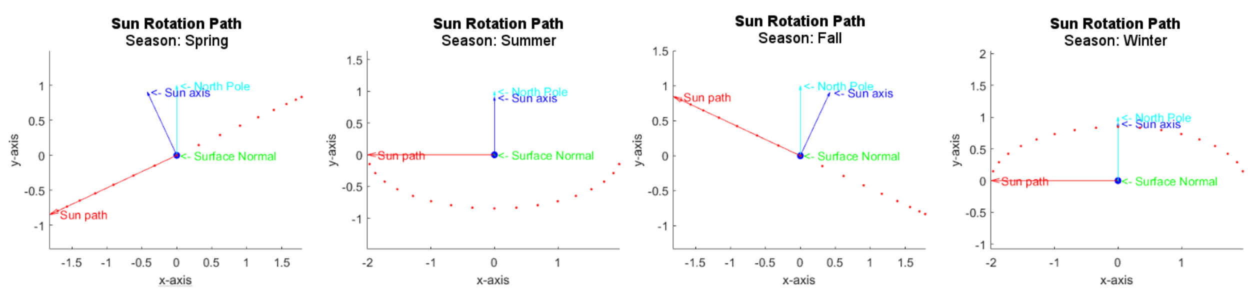

Figure 16: *Path of sun across Martian sky for differing seasons at proposed landing site.*

4.2. Spacecraft Dust Model

A numerical dust accumulation model was developed in order to test the solar array efficiency over long time spans in the Martian environment. Research showed that dust accumulated at a rate of about 0.28% per day, so this was used as the baseline for our accumulation model [18]. Dust coverage was applied on a daily basis as the incremental changes from hour to hour are negligible with yearlong time spans. The model aided us in predicting the total dust accumulation and reduction in solar cell efficiency due to this coverage effect. Additionally, the EDS dust abatement efficiency was included within the dust model. EDS cycles were scheduled for every 10 days as decreasing this interval yielded minimal abatement increases for the additional power cost. This would require a power of 120 kWh to operate over the duration of a Martian solar day (sol) for the entire solar panel surface area. A plot of the simulated dust accumulation on our solar array during a Martian year is showcased below in Figure 17.

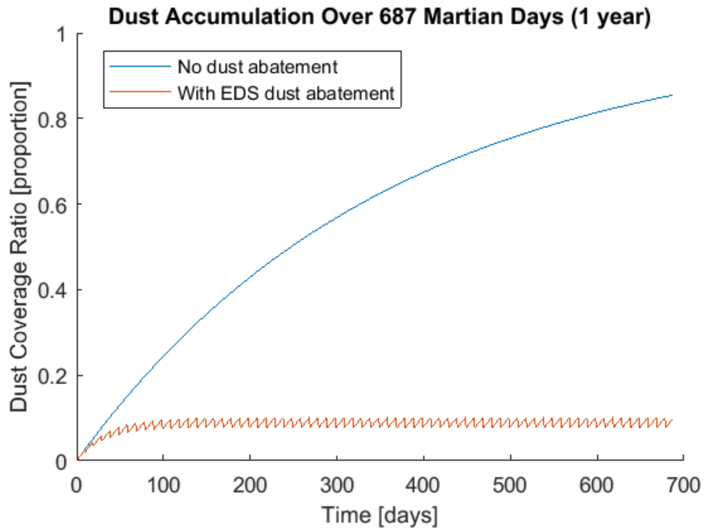

Figure 17: *Dust accumulation numerical model with and without EDS dust abatement active.*

In this figure, it is apparent that without dust abatement the dust accumulation on the surface of the solar panel becomes very severe over the span of a Martian year. However, with the EDS dust abatement active, the dust accumulation plateaus around 10% surface coverage. This dust abatement method would make APPA significantly more sustainable over long durations of time, and this model does not take into account the potential benefits of passive dust abatement by cleaning events discussed previously.

4.3. Power Output Analysis

As described in the solar cell design section, a representative cell currently used in space applications produced by Spectrolab provided the necessary variables to give a preliminary analysis of IMM technological potential in a Martian environment. The cell involves a triple junction composed of $GaInP_2/GaAs/Ge$. To begin the analysis, consider the general equation for power production of a solar system [19].

$$E = A * \eta_c * G * PR \quad \text{(Equation 5)}$$

Where E is power produced, A is solar cell area, η_C is the solar cell efficiency, G is average solar insolation, and PR is performance ratio. To determine the total power produced by the entire array, each umbrella was split into finite pieces, with the energy produced at a particular time of day assessed at each individual location. This technique was necessary due to the geometric challenge posed by the umbrella shape. Unlike a flat panel, the solar incidence angle over the conical surface of the umbrella is unique at each radial position. The umbrella surface was discretized as a pyramid with many sides which permitted power production estimations of each face of the pyramid. Thus, the total power production of the solar array is a summation of all these finite pieces. The area of the cell and average solar insolation are both fairly simple parameters to determine, as area is merely a property of umbrella geometry, and average solar insolation can be determined from the Martian Climate Database (MCD) for a particular location on the Martian surface [17]. Solar cell efficiency and performance ratio, on the other hand, are significantly more complex to determine.

Without experimental capabilities, determining solar cell efficiency is a complex task that utilizes theoretical equations tailored for particular solar cell designs. For any solar cell, temperature and solar concentration are the two most contributing factors for efficiency. Temperature follows a linear trend, where increasing temperature decreases efficiency. For a triple junction cell type, efficiency increases at a rate of 1 percent for every temperature drop of 20 °C [20]. Solar concentration, on the other hand, saw a fairly constant value with changing intensity, thus its effects were ignored.

Finally, performance ratio takes into account every potential loss that could reduce the overall power output of the array as a whole, ranging from dust coverage, shading, and electrical losses, among others. Electrical details involving inverters, cabling, and other necessary equipment are beyond the scope of this project, thus losses from this source were ignored. Shading effects were taken into account when calculating energy production of each discretized section of the umbrella, as any piece with an angle of incidence greater than 90° - therefore not receiving direct sunlight - was removed from the total energy summation. Therefore, the performance ratio used in this analysis will consist of the losses due to dust coverage and sub-optimal angles of solar incidence. The dust model was already demonstrated previously in the report, but Figure 18 demonstrates the calculated losses from suboptimal incidence angles.

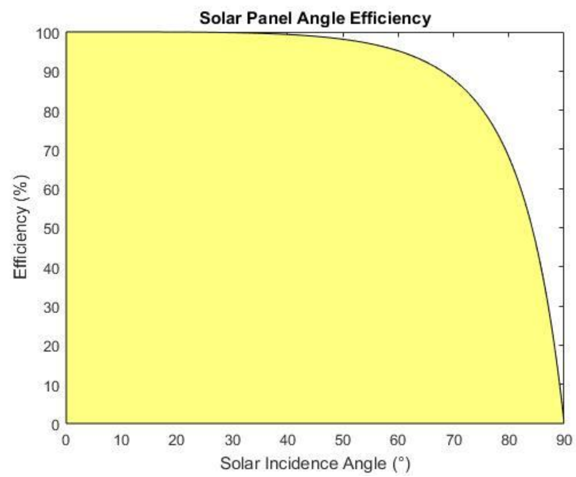

Figure 18: *Losses to power production from suboptimal incidence angles.*

The data presented in Figure 18 are based on reflection and scattering losses from ever increasing incidence angles. This is based on the refractive index of the anti-reflective coating described in the solar cell design compared to the refractive index of the Martian atmosphere [21]. When coupled with the sun rotation model and geometric discretization of the umbrella discussed previously, a method to model the power production losses from incidence angle variation was created. With all of these factors accounted for, Figure 19 demonstrates the daily power production curve for a single umbrella at a location of -5.064° latitude and 154.915° longitude (Aeolis/Zephyria Plana region). Temperature and solar flux values were provided by the MCD.

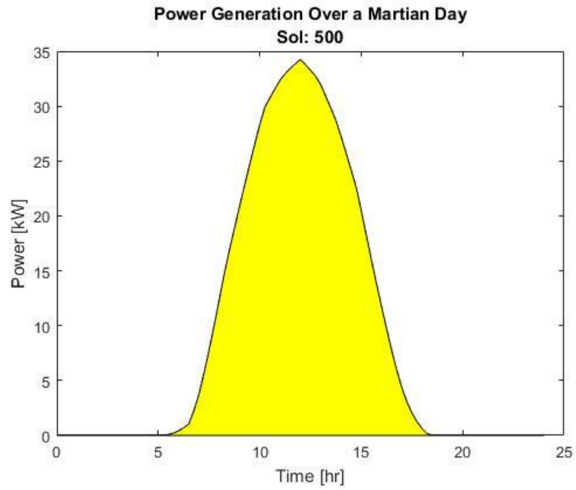

Figure 19: *Solar panel power generation over a Martian Sol.*

From Figure 19, the shading issues associated with APPA are apparent. Steep inclines and declines in the power production curve indicate limited power production during dusk and dawn, where only a fraction of the umbrella is exposed to the sun. Even so, an average power production of 9 kW per umbrella is generated across the day with a total of 37 kW for the entire array, assuming negligible differences between umbrellas. Total daily power production per umbrella is 228 kWh. For this demonstration, the effects of dust coverage are neglected, as no significant change in dust coverage would be observed hour-to-hour across a single day. Following the daily power production curve, a year-long calculation with day-to-day power production averages will take dust accumulation into account. Similarly, a demonstration of how APPA would operate in different latitudes and seasons is also shown in Figures 20-21, showing the yearly power production.

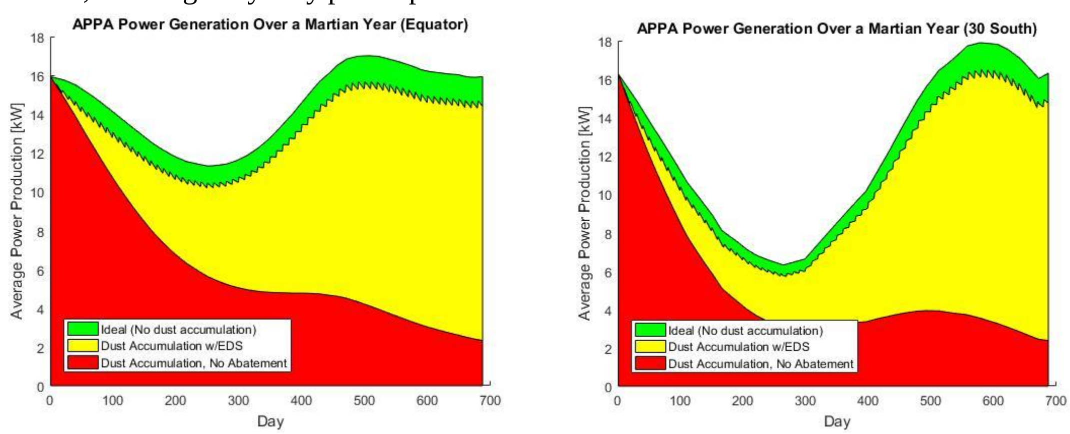

Figure 20: *Average daily power generation at the equator and 30° south across a Martian year.*

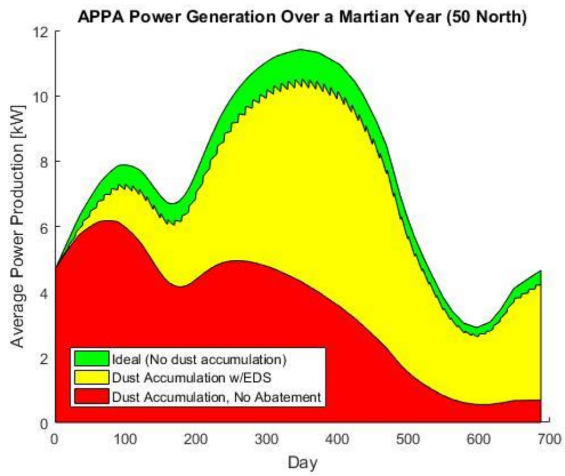

Figure 21: *Power generation at 50° north across a Martian year.*

Mirroring the data supplied from the challenge page regarding solar flux availability across a Martian year, Figures 20 and 21 gives insight into how APPA performs across the Martian landscape. An average temperature of -90 ℃ was assumed across the year, and each interpolated maximum solar flux value was reduced by a factor of 0.33 to reflect a closer average daily value. Both of those approximations were made based on information from the Martian Climate Database. The curves closer to the equator mostly follow the average solar surface flux; however, some variation does occur due to the variations in the sun's path across the sky due to the change in seasons. These variations hold increasingly significant effects on power production as latitude pushes farther from the equator. Daily average power production is 13 kW, 11 kW, and 7 kW for calculations at the Equator, 30° south, and 50° north respectively. Similarly, the total power generated on average per day is 321 kWh, 270 kWh, and 166 kWh, again for each corresponding location. Spikes in the dust accumulation with EDS is caused by the frequency at which the dust abatement system is activated, run for an entire 24 hour cycle every 10 days. Based on the EDS analysis earlier in the report, this energy consumption correlates to 125 kWh for the entire solar array throughout one cycle.

5. Conclusion

In order to facilitate a manned mission on Mars, producing consistent and reliable power is imperative. APPA has the potential to effectively fulfil this need by generating solar power while combating the harsh environment present on Mars. This design incorporates cutting edge technologies to reduce material weight and increase strength. The main solar array design deploys umbrella like structures covered in flexible, thin film solar cells. APPA also utilizes novel integration of electromagnetic linear actuation, which optimizes deployment of critical structures. These make the design lightweight, yet rigid and structurally safe, and require less power for operation. Interwoven tethers also allow for the resulting structure to remain in tension providing support to umbrellas and cantilevered booms. In order to ensure that the solar panels reliably generate energy, electrostatic waves are generated to pulse off the charged dust particles that have settled on the surface. This has the potential to supplement cleaning events to optimize the solar cells efficiency throughout its lifetime.

A comprehensive analysis of the validity of this design has been completed, including a finite element analysis for stress assessment and refinement. Proof of a generated dust model integrated into the SpaceCRAFT VR has showed the potential capabilities of the VR software to further refine the proposed design in the future. The models were also able to provide rough estimates of power generation for the solar cell array over the course of a Sol and a Martian year. As the perfect combination of strength, space efficiency, and sustainability, APPA represents the future for human exploration on Mars.

References

1. Landau, Elizabeth. “Phoenix.” *NASA Science: Solar System Exploration*, NASA's Science Mission Directorate, 25 Jan. 2018, solarsystem.nasa.gov/missions/phoenix/in-depth/.
2. “FuseBox.” *Essentium*, Essentium Materials LLC, 2017, essentiummaterials.com/fusebox/.
3. Rexroth Bosch Group. *Ball Transfer Units*, www.brtechnika.com/katalozi/pdf/Sachmeni_opori_2016_07.pdf.
4. Guter, Wolfgang, et al. “Current-Matched Triple-Junction Solar Cell Reaching 41.1% Conversion Efficiency under Concentrated Sunlight.” *Applied Physics Letters*, vol. 94, no. 22, 2009, p. 223504., doi:10.1063/1.3148341.
5. France, Ryan M., et al. “Design Flexibility of Ultrahigh Efficiency Four-Junction Inverted Metamorphic Solar Cells.” *IEEE Journal of Photovoltaics*, vol. 6, no. 2, 2016, pp. 578–583., doi:10.1109/jphotov.2015.2505182.
6. Kaltenbrunner, Martin, et al. "Flexible High Power-Per-Weight Perovskite Solar Cells with Chromium Oxide-Metal Contacts for Improved Stability in Air." *Nature Materials*, vol. 14, no. 10, Oct. 2015, pp. 1032-1039. EBSCO*host*, doi:10.1038/nmat4388.
7. “Photovoltaics.” *Spectrolab :: The World's Leading Provider of Compound Semiconductor and Lighting Products*, 2009, www.spectrolab.com/solarcells.htm.
8. Zhang, Zhitao, et al. “A Lightweight Polymer Solar Cell Textile That Functions When Illuminated from Either Side.” Angewandte Chemie, vol. 126, no. 43, 2014, pp. 11755–11758., doi:10.1002/ange.201407688.
9. Mather, Robert, and John Wilson. “Fabrication of Photovoltaic Textiles.” *Coatings*, vol. 7, no. 5, 2017, p. 63., doi:10.3390/coatings7050063.
10. Opwis, Klaus, et al. "Preparation of a Textile-Based Dye-Sensitized Solar Cell." *International Journal of Photoenergy*, 14 Aug. 2016, pp. 1-11. EBSCO*host*, doi:10.1155/2016/3796074.
11. Electronic Textiles : Smart Fabrics and Wearable Technology, edited by Tilak Dias, Elsevier Science, 2015. ProQuest Ebook Central, https://ebookcentral.proquest.com.ezproxy.library.tamu.edu/lib/tamucs/detail.action?docID=2039950.
12. “KEVLAR/Carbon Hybrid (Yellow).” *Fibre Glast Develpments Corporation*, Fibre Glast, www.fibreglast.com/product/kevlar-carbon-hybrid-yellow-1065/Kevlar.
13. Arbab, Alvira Ayoub, et al. “Multiwalled Carbon Nanotube Coated Polyester Fabric as Textile Based Flexible Counter Electrode for Dye Sensitized Solar Cell.” *Physical Chemistry Chemical Physics*, vol. 17, no. 19, 2015, pp. 12957–12969., doi:10.1039/c5cp00818b.
14. Yan, Xing, et al. “Enhanced Omnidirectional Photovoltaic Performance of Solar Cells Using Multiple-Discrete-Layer Tailored- and Low-Refractive Index Anti-Reflection Coatings.”*Advanced Functional Materials*, vol. 23, no. 5, 2012, pp. 583–590., doi:10.1002/adfm.201201032.
15. Beaty, Keith. “Formax Printing Solutions.” *Formax Printing*, 25 June 2014, www.formaxprinting.com/blog/2014/06/laminated-printing-choosing-a-laminate-thickness-to-fit-your-project/.
16. Sharma, Rajesh. “Experimental Evaluation and Analysis of Electrodynamic Screen as Dust Mitigation Technology for Future Mars Missions.” *IEEE Journals & Magazine*, vol. 45, no. 2, 16 Mar. 2009, doi:10.1109/TIA.2009.2013542.
17. Forget, FranÃ§ois, et al. “Improved General Circulation Models of the Martian Atmosphere from the Surface to above 80 Km.” *Journal of Geophysical Research: Planets*, vol. 104, no. E10, 1999, pp. 24155–24175., doi:10.1029/1999je001025.
18. Kerslake, Thomas W., and Lisa L. Kohout. “Solar Electric Power System Analyses for Mars Surface Missions.” *NASA*, NASA, 1 July 1999, ntrs.nasa.gov/search.jsp?R=19990063893.

19. “How to Calculate the Annual Solar Energy Output of a Photovoltaic System?” *How to Calculate the Output Energy or Power of a Solar Photovoltaic System, Excel PV Calculator to Estimate Solar Electricity Output.*, photovoltaic-software.com/PV-solar-energy-calculation.php.
20. Or, Assaf Ben, and Joseph Appelbaum. “Dependence of Multi-Junction Solar Cells Parameters on Concentration and Temperature.” *Solar Energy Materials and Solar Cells*, vol. 130, 2014, pp. 234–240., doi:10.1016/j.solmat.2014.07.010.
21. Wilson, A., and R. Ross. “Angle of Incidence Effects on Module Power and Energy Performance.”*Progress Report 21 and Proceedings of the 21st Project Integration Meeting*, 1983, pp. 423–426.